Amalgamating metalloligands with coordination networks†

Edwin C. Constable,* Guoqi Zhang, Catherine E. Housecroft* and Jennifer A. Zampese

Received 20th November 2009, Accepted 17th December 2009
First published as an Advance Article on the web 19th January 2010
DOI: 10.1039/b924475a

The O_4-cavity in [Cu{(*R*,*R*)-**1**}] ((*R*,*R*)-H_2**1** = 1,6-bis(3-ethoxy-2-hydroxyphenyl)-(3*R*,4*R*)-(−)-cyclohexane-1,2-diyl-2,5-diazahexa-1,5-diene) binds $HgBr_2$ to give *P*- and *M*-[Cu{(*R*,*R*)-**1**}$HgBr_2$]. In the solid state, there is no diastereoselectivity with respect to the handedness of the helical twist adopted by the coordinated Schiff base ligand and [Cu{(*R*,*R*)-**1**}$HgBr_2$] crystallizes with two independent molecules possessing *M*- and *P*-chirality, respectively, in the asymmetric unit. Single crystal structural data confirm that the same phenomenon is observed when [Ni{(*R*,*R*)-**1**}] is treated with $HgBr_2$or $Hg(CN)_2$. However, when an excess of $Hg(NO_3)_2{\cdot}H_2O$ reacts with [Cu{(*R*,*R*)-**1**}], *C*-mercuration occurs in both 3-ethoxy-2-hydroxyphenyl rings in addition to the coordination of a $Hg(NO_3)_2$ unit within the O_4-cavity of [Cu{(*R*,*R*)-**1**}]. This results in the formation of a two-dimensional coordination polymer network. The direct *C*-mercuration of a coordinated Schiff base ligand is not unique to the ligand in [Cu{(*R*,*R*)-**1**}], but also occurs during the reaction of [Cu(**3**)] (H_2**3** = 1,7-bis(3-ethoxy-2-hydroxyphenyl)- 2,6-diazahepta-1,6-diene) with $Hg(NO_3)_2{\cdot}H_2O$ proceeds in an analogous manner with *C*-mercuration occurs *para* to the phenolic oxygen atom.

Introduction

Our recent investigations of copper(II) complexes containing chiral Schiff base ligands[1-4] have illustrated the ability of the O_4-cavity in [Cu{(*R*,*R*)-**1**}] ((*R*,*R*)-H_2**1** = 1,6-bis(3-ethoxy-2-hydroxyphenyl)-(3*R*,4*R*)-(−)-cyclohexane-1,2-diyl-2,5-diazahexa-1,5-diene, Scheme 1) to engage in coordinate or hydrogen bond formation. Although similar observations have been described for a range of related complexes,[5] our principal interest focuses on chiral systems such as [Cu{(*R*,*R*)-**1**}], the catalytic activity of which may be tuned by the presence of a second metal ion.[1] Collectively, species of this type may be coined metalloligands as the complexes possess additional defined coordination capacity. Bu and coworkers[6] have reported a series of dimetallic complexes containing chiral salen-type ligands in which a Cu^{2+} ion is bound within the N_2O_2-cavity and an HgX_2 unit is coordinated by the *O*-donors (Scheme 2). Structural data for the chlorido complex confirmed that the complex is monomeric and that the $HgCl_2$ unit is raised out of the plane of the CuO_2-unit and is tilted to give a short Cu…Cl contact (Scheme 2).[6] Expanding the second binding pocket to an O_4-donor set (in this case with the achiral ligand H_2**2**, Scheme 3), and exploiting the hard–soft donor abilities of the thiocyanate ion, results in the formation of a one-dimensional coordination polymer in which copper(II) and mercury(II) centres are bridged by $[NCS]^-$ ligands.[7] The

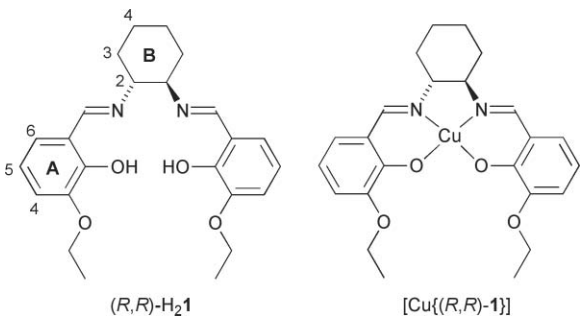

Scheme 1 Ligand **1** and its copper(II) complex.

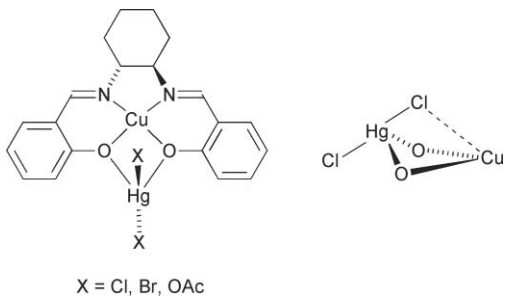

Scheme 2 One of the family of salen-type complexes reported by Bu, and the orientation of the $HgCl_2$ unit that generates a short Cu…Cl contact.[6]

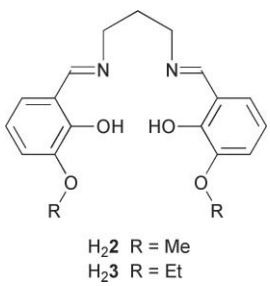

Scheme 3 Structures of ligands H_2**2** (used by Andruh[7]) and H_2**3**.

Department of Chemistry, University of Basel, Spitalstrassse 51, CH-4056, Basel, Switzerland. E-mail: catherine.housecroft@unibas.ch, edwin.constable@unibas.ch; Fax: +41 61 267 1018; Tel: +41 61 267 1008

† CCDC reference numbers 755410–755413. For crystallographic data in CIF or other electronic format see DOI: 10.1039/b924475a

selective binding of mercury(II) ions by compartmental Schiff base ligands containing appropriate fluorophores as auxillaries has been exploited for the development of fluorescent sensors for this toxic metal.[8]

In this work, we describe how the O_4-cavity in [Cu{(*R*,*R*)-**1**}] and [Ni{(*R*,*R*)-**1**}] binds $HgBr_2$ or $Hg(CN)_2$ in a predictable manner, whereas the reaction between [Cu{(*R*,*R*)-**1**}] or [Cu(**3**)] (H_2**3** = 1,7-bis(3-ethoxy-2-hydroxyphenyl)- 2,6-diazahepta-1,6-diene) with $Hg(NO_3)_2{\cdot}H_2O$ leads to unexpected *C*-mercuration of the 3-ethoxy-2-hydroxyphenyl rings and the formation of a two-dimensional network.

Experimental

IR spectra were recorded on a Shimadzu FTIR-8400S spectrophotometer with solid samples in a Golden Gate diamond ATR accessory. ^{1}H NMR spectra were recorded on Bruker DRX-500 NMR spectrometer; chemical shifts are referenced to residual solvent peaks (TMS = δ 0 ppm). Electronic absorption were recorded on a Varian-Cary 5000 spectrophotometer. Electrospray ionization (ESI) and fast atom bombardment (FAB) mass spectra were recorded on Bruker esquire 3000^{plus} and Finnigan MAT8400 mass spectrometers, respectively. Solvents were distilled before use, the water content being determined by Karl Fischer titration.

Ligands (*R*,*R*)-H_2**1**[3] and H_2**3**[9] were prepared as previously reported. *Toxicity warning*: all mercury salts are toxic and should be handled accordingly.

[Ni{(*R*,*R*)-**1**}]

(*R*,*R*)-H_2**1** (20.5 mg, 0.0500 mmol) was dissolved in a mixture of CH_2Cl_2–MeOH (15 cm^3, v/v, 2 : 1). Solid $Ni(OAc)_2{\cdot}4H_2O$ (12.4 mg, 0.0500 mmol) was added to the stirred solution of ligand, and the resulting red-brown solution was stirred for a further 10 min. The reaction mixture was filtered and the filtrate was allowed to evaporate slowly over 2 days during which time [Ni{(*R*,*R*)-**1**}] precipitated as red needles. These were collected by filtration, washed with EtOH and dried in air (yield: 18.8 mg, 81.0%). ^{1}H NMR (500 MHz, $CDCl_3$) δ/ ppm 7.28 (s, 2H, $H^{HC=N}$), 6.66 (d, J = 7.5 Hz, 2H, H^{A4}), 6.61 (d, J = 7.9 Hz, 2H, H^{A6}), 6.38 (t, J = 7.7 Hz, 2H, H^{A5}), 4.01 (m, 4H, $H^{Et\text{-}CH2}$), 3.13 (m, 2H, H^{B3}), 2.38 (m, 2H, H^{B2}), 1.87 (m, 2H, H^{B4}), 1.44 (t, J = 6.8 Hz, 6H, $H^{Et\text{-}CH3}$), 1.30 (m, 4H, $H^{B3'+B4'}$). ESI-MS (CH_2Cl_2–MeOH) m/z 489.2 [Ni(**1**) + Na]$^+$ (base peak, calc. 489.1), 955.4 [Ni_2(**1**)$_2$ + Na]$^+$ (calc. 955.3). Found C 61.41; H 6.16; N 6.02; $C_{24}H_{28}N_2NiO_4$ requires C 61.70; H 6.04; N 6.00%.

[Cu{(*R*,*R*)-**1**}$HgBr_2$]

Solid $Cu(OAc)_2$ (9.0 mg, 0.050 mmol) was added to a stirred solution of (*R*,*R*)-H_2**1** (20.5 mg, 0.0500 mmol) in a mixture of CH_2Cl_2 and MeOH (15 cm^3, v/v, 2 : 1) at room temperature. The resulting brown solution was stirred for 10 min, and then solid $HgBr_2$ (36.0 mg, 0.100 mmol) was added. After being stirred for a few minutes, the pale-brown solution was filtered, and the filtrate was allowed to evaporate slowly over two weeks at room temperature. The red block-like crystals of [Cu{(*R*,*R*)-**1**}$HgBr_2$] that formed were collected by filtration, washed with EtOH and dried in air (yield: 31.2 mg, 75.1%). FT-IR (solid, cm^{-1}): 2931w, 1626 s, 1599 s, 1550 m, 1465 s, 1437 s, 1391 m, 1347 m, 1311 s, 1292 m, 1242 s, 1217 s, 1177w, 1113 m, 1079 m, 1028 m, 1014w, 1003w, 904 m, 843 m, 783w, 770w, 747 m, 732 s, 635w. UV/VIS λ_{max}/nm (5.0×10^{-5} mol dm^{-3}, CH_2Cl_2) 238 (ε/10^3 dm^3 mol^{-1} cm^{-1} 52.9), 287 (29.0), 374 (8.56), 560 (0.302). ESI-MS (CH_2Cl_2–MeOH) m/z 494.2 [Cu(**1**) + Na]$^+$ (base peak, calc. 494.1), 965.5 [Cu_2(**1**)$_2$ + Na]$^+$ (calc. 965.3). FAB-MS m/z 472.1 [Cu(**1**) + H]$^+$ (base peak, calc. 472.1), 945.1 [Cu_2(**1**)$_2$ + H]$^+$ (calc. 945.3).

[Ni{(*R*,*R*)-**1**}$HgBr_2$]

The method was as for [Cu{(*R*,*R*)-**1**}$HgBr_2$], replacing $Cu(OAc)_2$ by $Ni(OAc)_2{\cdot}4H_2O$ (24.8 mg, 0.100 mmol). [Ni{(*R*,*R*)-**1**}$HgBr_2$] crystallized as red blocks over a period of one week. The crystals were collected by filtration, washed with EtOH, and dried in air (yield: 23.5 mg, 56.9%). ^{1}H NMR (500 MHz, $CDCl_3$) δ (ppm) 7.38 (s, 2H, $H^{HC=N}$), 6.75 (m, 4H, H^{A4+A6}), 6.54 (t, J = 7.8 Hz, 2H, H^{A5}), 4.17 (m, 4H, $H^{Et\text{-}CH2}$), 3.04 (m, 2H, H^{B3}), 2.44 (m, 2H, H^{B2}), 1.92 (m, 2H, H^{B4}), 1.60 (m, 6H, $H^{Et\text{-}CH3}$), 1.31 (m, 4H, $H^{B3'+B4'}$). FT-IR (solid, cm^{-1}): 2933w, 1623 s, 1601 s, 1553 m, 1465 s, 1447 s, 1393 m, 1347 m, 1311 s, 1293 m, 1245 s, 1226 s, 1178 m, 1105 m, 1081 m, 1039 m, 1017w, 963w, 899 m, 845w, 782w, 773 m, 744 m, 731 s, 656w. UV/VIS λ_{max}/nm (5.0×10^{-5} mol dm^{-3}, CH_2Cl_2) 235 (ε/10^3 dm^3 mol^{-1} cm^{-1} 43.5), 254 (49.5), 350 (10.1), 411 (5.98), 572 (0.122). ESI-MS (CH_2Cl_2–MeOH) m/z 489.2 [Ni(**1**) + Na]$^+$ (base peak, calc. 489.1), 955.7 [Ni_2(**1**)$_2$ + Na]$^+$ (calc. 955.3). FAB-MS m/z 467.1 [Ni(**1**) + H]$^+$ (base peak, calc. 467.1), 933.1 [Ni_2(**1**)$_2$ + H]$^+$ (calc. 933.3).

[Ni{(*R*,*R*)-**1**}$Hg(CN)_2$]

The method was as for [Ni{(*R*,*R*)-**1**}$HgBr_2$], replacing $HgBr_2$ by $Hg(CN)_2$ (25.4 mg, 0.100 mmol). [Ni{(*R*,*R*)-**1**}$Hg(CN)_2$] crystallized as yellow, thin plates from the CH_2Cl_2–MeOH filtrate over a period of one week at room temperature. The crystals were collected by filtration, washed with EtOH and dried in air (yield: 25.2 mg, 70.0%). ^{1}H NMR (500 MHz, $CDCl_3$) δ (ppm) 7.38 (s, 2H, $H^{HC=N}$), 6.76 (d, J = 7.8 Hz, 4H, H^{A4+A6}), 6.54 (t, J = 7.8 Hz, 2H, H^{A5}), 4.16 (m, 4H, $H^{Et\text{-}CH2}$), 3.06 (m, 2H, H^{B3}), 2.44 (m, 2H, H^{B2}), 1.92 (m, 2H, H^{B4}), 1.57 (t, J = 7.0 Hz, 6H, $H^{Et\text{-}CH3}$), 1.30 (m, 4H, $H^{B3'+B4'}$). FT-IR (solid, cm^{-1}): 2932w, 1631 s, 1603 s, 1553 m, 1466 s, 1447 s, 1393 m, 1343 m, 1311 s, 1293 s, 1245 s, 1228 s, 1174 m, 1105 m, 1085 s, 1041 m, 1020 m, 948w, 901 m, 846w, 806w, 770w, 736 s, 685w, 655w. UV/VIS λ_{max}/nm (5.0×10^{-5} mol dm^{-3}, CH_2Cl_2) 255 (ε/10^3 dm^3 mol^{-1} cm^{-1} 50.0), 274sh (23.1), 350 (10.1), 407 (5.96), 580 (0.094). ESI-MS (CH_2Cl_2–MeOH) m/z 489.1 [Ni(**1**) + Na]$^+$ (base peak, calc. 489.1), 955.7 [Ni_2(**1**)$_2$ + Na]$^+$ (calc. 955.3). FAB-MS m/z 467.1 [Ni(**1**) + H]$^+$ (base peak, calc. 467.1), 694.1 [NiHg(**1**)CN]$^+$ (calc. 694.1), 933.2 [Ni_2(**1**)$_2$ + H]$^+$ (calc. 933.3).

[Cu{(*R*,*R*)-**1**–2H}{$Hg(ONO_2)_2$}{$Hg(ONO_2)$}$_2$]$_n$

Solid $Cu(OAc)_2$ (9.0 mg, 0.050 mmol) was added to a stirred solution of (*R*,*R*)-H_2**1** (20.5 mg, 0.0500 mmol) in a mixture of CH_2Cl_2 and MeOH (15 cm^3, v/v, 2 : 1). The brown solution was stirred for 10 min, after which time $Hg(NO_3)_2{\cdot}H_2O$ (68.8 mg, 0.200 mmol) was added. Once this salt had completely dissolved, the resulting pale-brown solution was filtered. The filtrate was left to stand at room temperature for one week, during which time brown needle-like crystals formed. These were collected by filtration, washed with EtOH and dried in air (yield: 54.3 mg,

82.1%). FT-IR (solid, cm^{-1}): 2938w, 1625 m, 1506 m, 1447 s, 1381w, 1303 m, 1261 s, 1221 s, 1091 m, 1022 m, 991 m, 969 m, 904w, 857w, 795w, 777w, 740 m, 706w, 662w. Found C 23.65; H 2.40, N 6.05%; $C_{24}H_{26}CuHg_3N_6O_{16}$·1.5EtOH requires C 23.35; H 2.54, N 6.05%.

[Cu(3–2H){Hg(ONO$_2$)$_2$}{Hg(ONO$_2$)}$_2$]$_n$

Solid $Cu(OAc)_2$ (9.0 mg, 0.05 mmol) was added to a stirred solution of H_2**3** (18.5 mg, 0.05 mmol) in CH_2Cl_2–MeOH (15 cm^3, v/v, 2 : 1) at room temperature. After the brown solution had been stirred for 10 min, $Hg(NO_3)_2$·H_2O (68.8 mg, 0.20 mmol) was added and the reaction mixture stirred until all solid had dissolved. The green solution was filtered, and after allowing the filtrate to stand for a week at room temperature, the green needle-like crystals that formed were collected by filtration. The crystals were washed with EtOH and dried in air (yield: 51.5 mg, 80.3%). FT-IR (solid, cm^{-1}): 2929w, 1616 s, 1507 m, 1456 s, 1388w, 1267 s, 1225 s, 1095w, 1069 m, 1010 m, 968 m, 905w, 860w, 794w, 778w, 742 m, 683w, 668w.

Crystal structure determinations†

Data were collected on a Stoe IPDS diffractometer. The data reduction, solution and refinement used Stoe IPDS software[10] and the program SHELXL97.[11] ORTEP figures were drawn using Ortep-3 for Windows.[12] Structures have been analysed using Mercury v. 2.2.[13]

[Cu{(*R*,*R*)-1}HgBr$_2$]

$C_{24}H_{28}Br_2CuHgN_2O_4$, $M = 832.42$, red block, monoclinic, space group $P2_1$, $a = 11.0988(9)$, $b = 17.2977(10)$, $c = 14.2186(11)$ Å, $\beta = 106.704(3)°$, $U = 2614.6(3)$ Å^3, $Z = 4$, $D_c = 2.115$ Mg m^{-3}, μ(Mo-Kα) = 9.767 mm^{-1}, $T = 173$ K. Total 120170 reflections, 12853 unique, $R_{int} = 0.1385$. Refinement of 12799 reflections (617 parameters) with $I > 2\sigma(I)$ converged at final $R_1 = 0.0307$ ($R1$ all data = 0.0309), w$R_2 = 0.0821$ ($wR2$ all data = 0.0822), gof = 1.126.

[Ni{(*R*,*R*)-1}HgBr$_2$]

$C_{24}H_{28}Br_2HgN_2NiO_4$, $M = 827.56$, red block, monoclinic, space group $P2_1$, $a = 11.0776(12)$, $b = 17.2924(13)$, $c = 14.1961(14)$ Å, $\beta = 107.220(8)°$, $U = 2597.5(4)$ Å^3, $Z = 4$, $D_c = 2.116$ Mg m^{-3}, μ(Mo-Kα) = 9.738 mm^{-1}, $T = 173$ K. Total 43549 reflections, 10176 unique, $R_{int} = 0.0681$. Refinement of 10046 reflections (618 parameters) with $I > 2\sigma(I)$ converged at final $R_1 = 0.0285$ ($R1$ all data = 0.0291), w$R_2 = 0.0709$ ($wR2$ all data = 0.0712), gof = 1.140.

[Ni{(*R*,*R*)-1}Hg(CN)$_2$]

$C_{26}H_{28}HgN_4NiO_4$, $M = 719.80$, yellow plate, orthorhombic, space group $P2_12_12_1$, $a = 13.623(3)$, $b = 14.347(3)$, $c = 26.022(5)$ Å, $U = 5086.2(18)$ Å^3, $Z = 8$, $D_c = 1.880$ Mg m^{-3}, μ(Mo-Kα) = 6.810 mm^{-1}, $T = 173$ K. Total 125195 reflections, 9989 unique, $R_{int} = 0.2027$. Refinement of 9934 reflections (654 parameters) with $I > 2\sigma(I)$ converged at final $R_1 = 0.0526$ ($R1$ all data = 0.0528), w$R_2 = 0.1389$ ($wR2$ all data = 0.1391), gof = 1.140.

[Cu{(*R*,*R*)-1–2H}{Hg(ONO$_2$)$_2$}{Hg(ONO$_2$)}$_2$]$_n$

$C_{48}H_{52}Cu_2Hg_6N_{12}O_{32}$, $M = 2639.66$, brown needle, monoclinic, space group $P2_1$, $a = 17.070(3)$, $b = 9.5066(19)$, $c = 20.658(4)$ Å, $\beta = 110.808(30)°$, $U = 3133.6(12)$ Å^3, $Z = 2$, $D_c = 2.798$ Mg m^{-3}, μ(Mo-Kα) = 15.408 mm^{-1}, $T = 173$ K. Total 62656 reflections, 11174 unique, $R_{int} = 0.1877$. Refinement of 10773 reflections (906 parameters) with $I > 2\sigma(I)$ converged at final $R_1 = 0.0608$ ($R1$ all data = 0.0622), w$R_2 = 0.1610$ ($wR2$ all data = 0.1627), gof = 1.051.

Results and discussion

The complex [Cu{(*R*,*R*)-**1**}] was prepared *in situ* by the reaction between equimolar amounts of $Cu(OAc)_2$ and (*R*,*R*)-H_2**1**.[3] The reaction was complete within 10 min, after which time $HgBr_2$ was added. Over a period of two weeks, red block-like crystals grew. The ESI mass spectra of these red blocks were inconclusive as regards the presence of mercury, only showing peaks that could be assigned to [Cu{(*R*,*R*)-**1**}] combined with Na^+. In the FAB mass spectrum, the base peak appeared at m/z 472.1 arising from [Cu(**1**) + H]$^+$ and a low intensity peak envelope at m/z 945.1 was assigned to [Cu$_2$(**1**)$_2$ + H]$^+$. The isotope pattern matched that simulated. Again, no peaks corresponding to mercury-containing ions were observed. An X-ray quality crystal was selected from the bulk sample and structural elucidation confirmed that the complex was [Cu{(*R*,*R*)-**1**}$HgBr_2$]. The compound crystallizes in the chiral space group $P2_1$, with two independent molecules in the asymmetric unit. The bond parameters for both are similar and one molecule is depicted in Fig. 1. As expected, the Cu^{2+} ion is bound within the N_2O_2-donor set. The $HgBr_2$ unit is coordinated by four *O*-donors, two at distances of 2.509(4) and 2.548(4) Å, and two weaker interactions with Hg–O distances of 2.813(5) and 2.838(4). In the second molecule, the corresponding distances are 2.504(4), 2.533(4), 2.831(4) and 2.786(4) Å. The coordination environment of the mercury centre resembles that shown in Scheme 2 for the salen-type complex structurally characterized by Bu,[6] but with two additional, longer range Hg···O contacts. The coordinated Schiff base ligand adopts a helical twist, the handedness of which is different in each of the two independent molecules. The diastereoisomers containing Hg1a and Hg1b are of *M*- and *P*-chirality, respectively (Fig. 2). In the solid state, therefore, there is no diastereoselectivity with respect to the helical encapsulation of the mercury(II) centre.

The red nickel(II) complex [Ni{(*R*,*R*)-**1**}] is formed in 81% yield by the reaction between $Ni(OAc)_2$·$4H_2O$ and (*R*,*R*)-H_2**1**. The ^{1}H NMR spectrum of a $CDCl_3$ solution of the complex is consistent with a diamagnetic species and, therefore, a square-planar environment for the Ni^{2+} ion. The symmetrical nature of the spectrum (assigned by COSY and NOESY techniques) shows that in solution the complex is symmetrical. The base peak in the electrospray mass spectrum (m/z 489.2) corresponded to [Ni(**1**) + Na]$^+$ while the highest mass peak envelope at m/z 955.4 was assigned to [Ni$_2$(**1**)$_2$ + Na]$^+$.

The *in situ* preparation of [Ni{(*R*,*R*)-**1**}], followed by reaction with $HgBr_2$ or $Hg(CN)_2$, produced ruby-red crystals of [Ni{(*R*,*R*)-**1**}$HgBr_2$] or yellow plate-like crystals of [Ni{(*R*,*R*)-**1**}Hg(CN)$_2$], respectively. Despite the different colours in the solid state, both nickel(II) complexes dissolve in CH_2Cl_2 to give yellow solutions.

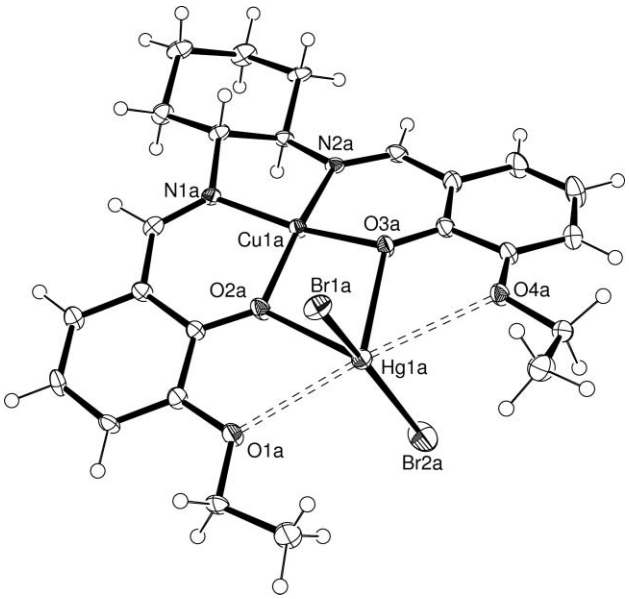

Fig. 1 Structure of one of the two independent molecules of [Cu{(*R*,*R*)-**1**}$HgBr_2$] in the asymmetric unit (ellipsoids plotted at 40% probability level). Selected bond parameters: Cu1a-O2a = 1.895(4), Cu1a-O3a = 1.901(4), Cu1a-N2a = 1.919(4), Cu1a-N1a = 1.927(4), Hg1a-Br2a = 2.4489(7), Hg1a-Br1a = 2.4527(7), Hg1a-O2a = 2.509(4), Hg1a-O3a = 2.548(4), Hg1a-O1a = 2.813(5), Hg1a-O4a = 2.838(4) Å; O2a-Cu1a-O3a = 89.46(18), O3a-Cu1a-N2a = 93.99(19), O2a-Cu1a-N1a = 94.23(19), N2a-Cu1a-N1a = 85.11(19), Br2a-Hg1a-Br1a = 158.85(3), O2a-Hg1a-O3a = 63.77(13), Br2a-Hg1a-O2a = 105.75(11), Br1a-Hg1a-O2a = 93.41(11), Br2a-Hg1a-O3a = 96.28(10), Br1a-Hg1a-O3a = 100.25(10)°.

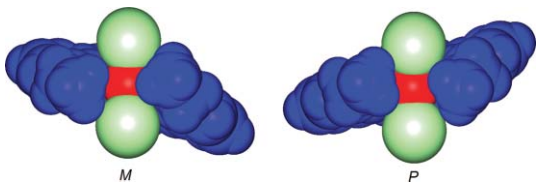

Fig. 2 The two independent molecules of [Cu{(*R*,*R*)-**1**}$HgBr_2$]. Those containing Hg1a (left) and Hg1b (right) are of *M*- and *P*-chirality, respectively (Hg, red; Br, green; [Cu{(*R*,*R*)-**1**}], blue).

Fig. 3 illustrates the similarity of the solution UV-VIS spectra of [Ni{(*R*,*R*)-**1**}$HgBr_2$] and [Ni{(*R*,*R*)-**1**}$Hg(CN)_2$], and compares them to that of [Cu{(*R*,*R*)-**1**}$HgBr_2$], a CH_2Cl_2 solution of which appears red. Each complex exhibits a weak MLCT absorption around 560-570 nm, but in the case of the nickel(II) complexes, a significantly more intense absorption appears close to 410 nm and leads to the observed yellow colour in solution. As in the case of [Cu{(*R*,*R*)-**1**}$HgBr_2$], the ESI mass spectra of the nickel(II) complexes provided no evidence for the presence of mercury, and only exhibited peaks arising from [Ni(**1**) + Na]$^+$ and [Ni_2(**1**)$_2$ + Na]$^+$. However, a peak arising from [NiHg(**1**)CN]$^+$ (*m*/*z* 694.1) was observed in the FAB mass spectra of [Ni{(*R*,*R*)-**1**}$Hg(CN)_2$]. Only small changes in the $CDCl_3$ solution ^{1}H NMR spectra were observed upon going from [Ni{(*R*,*R*)-**1**}] to the mercury-containing complexes. The signal for the imine proton shifted from δ 7.28 to 7.38 ppm, while signals for the phenyl ring protons all shifted slightly to higher frequency.

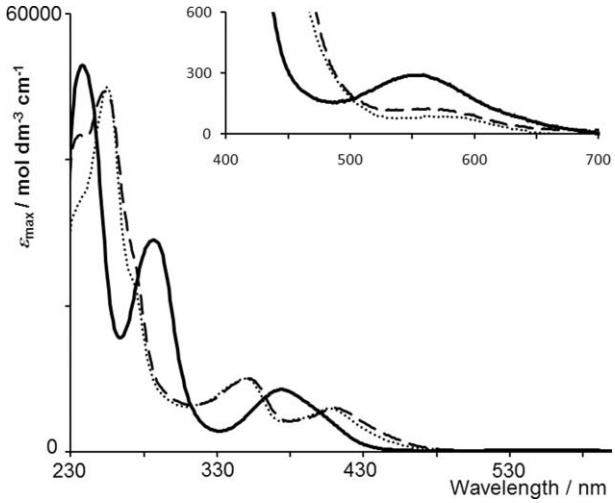

Fig. 3 UV-VIS spectra of CH_2Cl_2 solutions (5.0×10^{-5} mol dm^{-3}) of [Cu{(*R*,*R*)-**1**}$HgBr_2$] (—), [Ni{(*R*,*R*)-**1**}$HgBr_2$] (---) and [Ni{(*R*,*R*)-**1**}-$Hg(CN)_2$] (···).

Single crystals of [Ni{(*R*,*R*)-**1**}$HgBr_2$] and [Ni{(*R*,*R*)-**1**}$Hg(CN)_2$] were chosen from the bulk samples. The solid state structure of the bromido complex proved to be isomorphous with that of [Cu{(*R*,*R*)-**1**}$HgBr_2$] (the Ni–O and Ni–N bond distances are in the range 1.840(4) and 1.860(4) Å compared to a range of 1.893(4) and 1.937(4) Å for the corresponding Cu–O and Cu–N bond lengths). Once again, therefore, the structure contains two independent molecules having *P*- and *M*-chirality arising from the twist of the Schiff base ligand, and crystallization was non-diastereoselective. An analogous situation was observed in the solid state structure of [Ni{(*R*,*R*)-**1**}$Hg(CN)_2$]. The compound crystallizes in space group $P2_12_12_1$ with two independent molecules in the asymmetric unit, one of which is shown in Fig. 4. The diastereoisomer containing Hg1a (Fig. 4) has *P*-chirality while that containing Hg1b possesses *M*-chirality. The structure confirms the location of the Ni^{2+} ion within the N_2O_2-cavity and the $Hg(CN)_2$ unit within the O_4-domain. As in [M{(*R*,*R*)-**1**}$HgBr_2$] (M = Cu or Ni), the Hg(II) centre associates with the *O*-donors through two short and two long contacts. The caption to Fig. 4 gives the bond parameters for the molecule containing Hg1a, and for the second molecule the Hg1b–O distances are 2.524(4), 2.535(4), 2.721(4) and 2.774(6) Å. In each of [Cu{(*R*,*R*)-**1**}$HgBr_2$], [Ni{(*R*,*R*)-**1**}$HgBr_2$] and [Ni{(*R*,*R*)-**1**}$Hg(CN)_2$], the pairs of *P*- and *M*-diastereoisomers are closely associated through face-to-face π-interactions involving the phenyl rings and adjacent chelate ring. The interactions are most efficient in [Ni{(*R*,*R*)-**1**}$Hg(CN)_2$] in which the phenyl rings containing atoms C17a and C4b in adjacent *P*- and *M*-diastereoisomers overlap at a separation of 3.40 Å (Fig. 5). Although the salen-type complex structurally characterized by Bu (Scheme 2, X = Cl)[6] also crystallizes with two independent molecules in the asymmetric unit, inspection of the structure (refcode EQUHUT, accessed using Conquest v. 1.11[13]) confirmed that neither molecule has a well-developed helical twist. The structure of this $HgCl_2$-containing complex (Scheme 2) differs significantly from those of [Ni{(*R*,*R*)-**1**}$HgBr_2$], [Ni{(*R*,*R*)-**1**}$Hg(CN)_2$] and [Cu{(*R*,*R*)-**1**}$HgBr_2$] in that the $HgCl_2$ unit is tilted towards the copper(II) centre so that there is a short Cu···Cl contact. This results in a shorter Cu···Hg separation

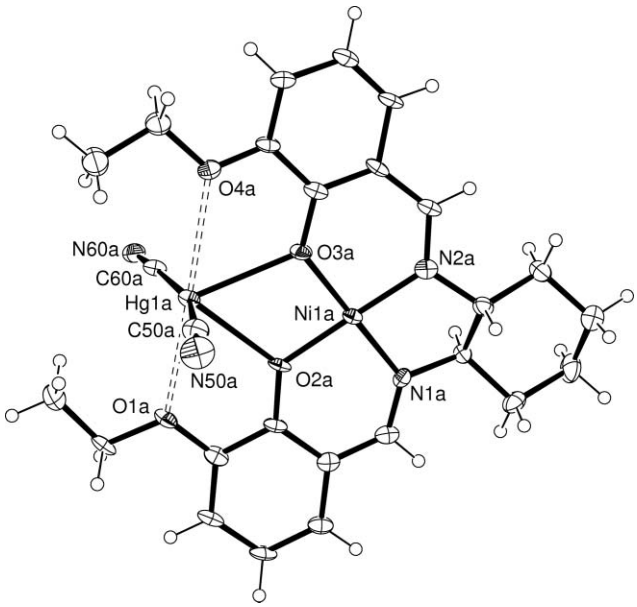

Fig. 4 Structure of one of the two independent molecules of [Ni{(*R*,*R*)-**1**}Hg(CN)$_2$] in the asymmetric unit (ellipsoids plotted at 40% probability level). Selected bond parameters: Ni1a-N1a = 1.846(5), Ni1a-N2a = 1.853(5), Ni1a-O3a = 1.859(4), Ni1a-O2a = 1.861(4), Hg1a-O2a = 2.531(4), Hg1a-O3a = 2.541(4), Hg1a-O1a = 2.723(4), Hg1a-O4a = 2.763(6), Hg1a-C50a = 2.047(7), Hg1a-C60a = 2.066(7), C50a-N50a = 1.142(10), N60a-C60a = 1.128(9) Å; N1a-Ni1a-N2a = 85.2(2), N2a-Ni1a-O3a = 94.7(2), N1a-Ni1a-O2a = 94.4(2), O3a-Ni1a-O2a = 85.8(2), C50a-Hg1a-C60a = 162.6(3), C50a-Hg1a-O2a = 95.7(2), C60a-Hg1a-O2a = 98.7(2), C50a-Hg1a-O3a = 96.8(2), C60a-Hg1a-O3a = 98.8(2), O2a-Hg1a-O3a = 59.91(14)°.

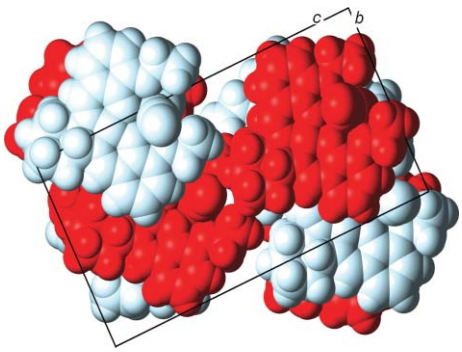

Fig. 5 Packing of pairs of *P*- and *M*-diastereoisomers (red and pale blue, respectively) in the unit cell of [Ni{(*R*,*R*)-**1**}Hg(CN)$_2$].

(3.2715(4) and 3.2750(14) Å in the two independent molecules) than in [Cu{(*R*,*R*)-**1**}HgBr$_2$] (3.4952(7) and 3.4999(7) Å for the independent molecules). The Ni…Hg separations in [Ni{(*R*,*R*)-**1**}HgBr$_2$] (3.5292(7) and 3.5195(8) Å) and [Ni{(*R*,*R*)-**1**}Hg(CN)$_2$] (3.5581(10) and 3.5597(10) Å) are slightly longer than the Cu···Hg distance in [Cu{(*R*,*R*)-**1**}HgBr$_2$].

We next chose to look at the reaction of [Cu{(*R*,*R*)-**1**}] with Hg(NO$_3$)$_2$·H$_2$O with the expectation that the variety of coordination modes possible for the nitrate ions might lead to structural modification of the [M{(*R*,*R*)-**1**}HgX$_2$] complex. When [Cu{(*R*,*R*)-**1**)}] (made *in situ*) was treated with one equivalent of Hg(NO$_3$)$_2$·H$_2$O, and the filtered reaction mixture was left to stand at room temperature, no solid precipitated. When the solvent was evaporated, only an oily residue could be isolated. However, when the amount of Hg(NO$_3$)$_2$·H$_2$O was increased (> two equivalents with respect to [Cu{(*R*,*R*)-**1**)}]), a brown crystalline product was obtained. The synthesis was optimized with four equivalents of Hg(NO$_3$)$_2$·H$_2$O. The compound was insoluble in common organic solvents and no ESI mass spectrometric data could be obtained. An X-ray quality crystal was selected from the bulk sample and structural analysis revealed the formation of the coordination polymer [Cu{(*R*,*R*)-**1**–2H}{Hg(ONO$_2$)$_2$}{Hg(ONO$_2$)}$_2$]$_n$. Fig. 6 illustrates one of the two independent units present in the asymmetric unit. The basic building block was the anticipated [Cu{(*R*,*R*)-**1**}{Hg(O$_2$NO)$_2$}] complex, but unexpectedly, the phenyl rings of the Schiff base ligand had undergone *C*-mercuration at the positions *para* to the phenoxy substituents. The second independent unit (containing atoms Cu1b, Hg1b, Hg2b and Hg3b) is structurally similar to the first and the two units are closely associated through two long Hg–O contacts (Hg3a–O10b = 2.715(18) and Hg2b–O10a = 2.675(18) Å) across a pseudo-inversion centre. This arrangement also allows the phenyl rings containing atoms C21a and C7b to engage in π-stacking (distance between rings = 3.58 Å), although the rings are not optimally positioned with repect to one another. The coordination environment of each copper(II) centre is as expected within the N_2O_2-cavity.

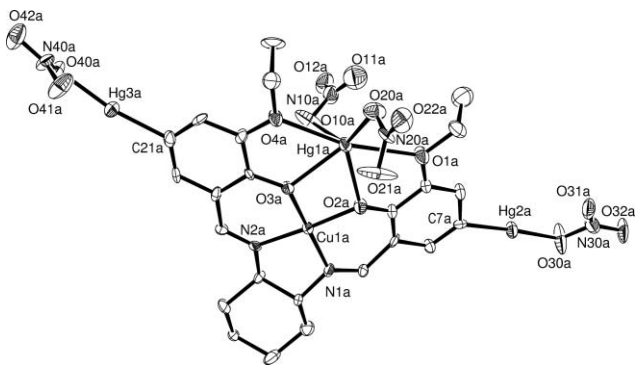

Fig. 6 Structure of one of the two independent units in [Cu{(*R*,*R*)-**1**–2H}{Hg(ONO$_2$)$_2$}{Hg(ONO$_2$)}$_2$]$_n$ (ellipsoids plotted at 35% probability level); H atoms are omitted for clarity. Selected bond parameters: Hg1a-O20a = 2.160(14), Hg1a-O2a = 2.335(12), Hg1a-O3a = 2.341(10), Hg1a-O10a = 2.379(19), Hg1a-O4A = 2.597(11), Hg1a-O1a = 2.623(12), Hg2a-C7a = 2.044(16), Hg2a-O30a = 2.045(13), Hg3a-C21a = 2.068(16), Hg3a-O40a = 2.136(12), Cu1a-O3a = 1.890(10), Cu1a-O2a = 1.906(11), Cu1a-N1a = 1.917(12), Cu1a-N2a = 1.935(12) Å; O1a-Hg1a-O2a = 63.2(4), O2a-Hg1a-O3a = 67.2(4), O3a-Hg1a-O4a = 63.7(4), O4a-Hg1a-O1a = 165.5(4), O20a-Hg1a-O10a = 131.5(6), O20a-Hg1a-O2a = 132.5(5), O2a-Hg1a-O10a = 92.1(6), C7a-Hg2a-O30a = 176.2(8), C21a-Hg3a-O40a = 170.0(6), O3a-Cu1a-O2a = 85.9(5), O2a-Cu1a-N1a = 93.0(5), O3a-Cu1a-N2a = 95.0(5), N1a-Cu1a-N2a = 86.8(5)°.

The solid state assembly in [Cu{(*R*,*R*)-**1**–2H}{Hg(ONO$_2$)$_2$}-{Hg(ONO$_2$)}$_2$]$_n$ can be considered, first, in terms of the evolution of chains and, second, the connection of these chains into sheets which lie in the *ab* plane. The chains are generated by O31a–Cu1b^{i}, O21a–Hg3b^{i}, O42b–Cu1a^{ii} and O21b–Hg2a^{ii} interactions (2.651(18), 2.92(2), 2.597(16) and 2.75(3) Å; symmetry codes *i* = 1+*x*, −1+*y*, *z*; ii = −1+*x*, 1+*y*, *z*). The parallel chains are

interconnected by Hg–O–Hg links (Hg1a–O11a–Hg3b^{iii}, 2.74(3) and 3.01(3) Å, 156.5(8)°, symmetry code iii = 1+x, y, z). All the Hg–O separations involved in this assembly are moderately long, but may be considered as legitimate attractive interactions that support the network. The sum of the van der Waals radii of Hg and O is 2.95 Å. Fig. 7 illustrates part of one of the sheets, and the projection is chosen so as to give a clear view of the propagation of the chains which run from left-to-right across figure. Fig. 8 illustrates the packing of sheets in the lattice. The nitrato-*O* atoms O22a point above and below the sheets but the closest O…Hg contacts are 3.17 Å (O22a…Hg3a^{iv}, symmetry code iv = 3–x, $-^1/_2+y$, 2–z). The distance is slightly too long to justify describing the structure in terms of a three-dimensional, rather than two-dimensional, network.

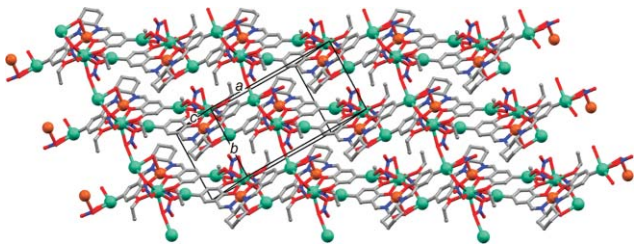

Fig. 7 Part of one sheet in the solid state structure of [Cu{(*R*,*R*)-**1**–2H}{Hg(ONO$_2$)$_2$}{Hg(ONO$_2$)}$_2$]$_n$. Colour code: Hg, green; Cu, orange; O, red; N, blue; C, grey (H atoms omitted).

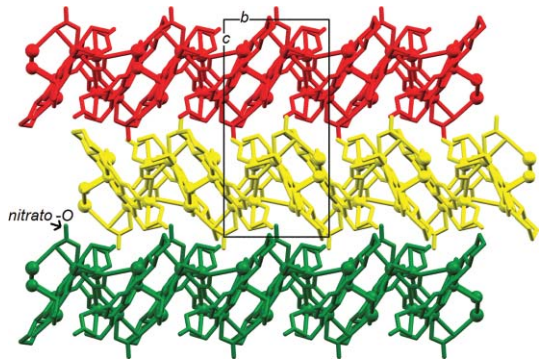

Fig. 8 Packing of two-dimensional sheets (each in the *ab* plane) in [Cu{(*R*,*R*)-**1**–2H}{Hg(ONO$_2$)$_2$}{Hg(ONO$_2$)}$_2$]$_n$.

The observation of *C*-mercuration which leads to the assembly of the polymeric structure of [Cu{(*R*,*R*)-**1**–2H}{Hg(ONO$_2$)$_2$}{Hg(ONO$_2$)}$_2$]$_n$ was not anticipated. To test whether this was confined to the reaction of [Cu{(*R*,*R*)-**1**}] with Hg(NO$_3$)$_2$·H$_2$O, we also investigated the reaction of a related copper(II) Schiff base complex with the same mercury(II) salt. We chose the achiral ligand H$_2$**3** which has the same two N_2O_2- and O_4-donor sets as (*R*,*R*)-H$_2$**1**. The reaction of Cu(OAc)$_2$, ligand H$_2$**3** and Hg(NO$_3$)$_2$·H$_2$O (1 : 1 : 4 molar equivalents) under the same conditions as used for ligand (*R*,*R*)-H$_2$**1** resulted in the isolation of green needle-like crystals. A preliminary data set for the complex confirmed the formation of the [Cu(**3**–2H){Hg(ONO$_2$)$_2$}{Hg(ONO$_2$)}$_2$]$_n$ with the same structural features as [Cu{(*R*,*R*)-**1**–2H}{Hg(ONO$_2$)$_2$}{Hg(ONO$_2$)}$_2$]$_n$. Unfortunately, several attempts to obtain a good quality data set were unsuccessful. Nonetheless, the results were sufficient to confirm that *C*-mercuration in the sites *para* to the two phenoxy substituents had again occurred. Attempts to investigate the reaction of [Cu{(*R*,*R*)-**1**}] and Hg(OAc)$_2$ gave a solid product, but no X-ray quality crystals could be obtained.

Although the formation of Hg–C$_{aryl}$ bonds often involves the use of organolithium or Grignard reagents,[14] direct mercuration using mercury(II) salts occurs if the substrate contains suitably acidic hydrogen atoms.[15] The mercuration of a coordinated ligand bearing acidic hydrogen atoms is exemplified by the reaction of HgBr$_2$ with [NiL] where L^{2-} is a tetraaza macrocyclic ligand produced by the metal-templated condensation of acetylacetone and 1,2-diaminobenzene. In this case, the first example of its type, mercuration occurs at the central carbon atom of each diiminate chelate ring.[16] Related to this is a rare example of the mercuration of a platinum(II)-bound [acac]$^-$ ligand.[17] As far as we are aware, however, mercuration at an arene CH unit of a coordinated ligand is highly unusual, one example being the mercuration of [CuL$_2$] (HL = 8-hydroxyquinoline) which undergoes a number of electrophilic substitution reactions.[18,19] For organic arenes, direct mercuration is common, and the salts typically chosen are mercury(II) chloride, acetate, trifluoroacetate or nitrate. In the early 1950s, it was shown that the rate of mercuration of benzene in aqueous solution is anion dependent. Chloride ions strongly inhibit the reaction, while nitrate and perchlorate ions increase the rate.[20] We conclude that this same anion dependence is responsible for the observed difference between the reactivity of [Cu{(*R*,*R*)-**1**}] with HgBr$_2$ or Hg(CN)$_2$, compared to that with Hg(NO$_3$)$_2$.

Conclusions

In this study, we have shown that the O_4-cavity in [Cu{(*R*,*R*)-**1**}] binds HgBr$_2$ to give *P*- and *M*-[Cu{(*R*,*R*)-**1**}HgBr$_2$]. Although ligand **1** is enantiomerically pure, crystallization of the product shows no discrimination with respect to the handedness of the helical twist adopted by the coordinated Schiff base ligand and [Cu{(*R*,*R*)-**1**}HgBr$_2$] crystallizes with two independent molecules possessing *M*- and *P*-chirality, respectively, in the asymmetric unit. This same trend is observed in the reactions of [Ni{(*R*,*R*)-**1**}] with HgBr$_2$ or Hg(CN)$_2$. However, when Hg(NO$_3$)$_2$·H$_2$O reacts with [Cu{(*R*,*R*)-**1**}], *C*-mercuration occurs in both 3-ethoxy-2-hydroxyphenyl rings in addition to the coordination of a Hg(NO$_3$)$_2$ moiety within the O_4-cavity of [Cu{(*R*,*R*)-**1**}]. This results in the formation of a two-dimensional coordination polymer network. The direct *C*-mercuration of a coordinated Schiff base ligand by a mercury(II) salt appears to be an unprecedented observation. However, it is not unique to the copper(II)-coordinated ligand [(*R*,*R*)-**1**]$^{2-}$. The reaction of [Cu(**3**)] with Hg(NO$_3$)$_2$·H$_2$O proceeds in an analogous manner with *C*-mercuration occurring at each site *para* to a phenoxy substituent.

Acknowledgements

We thank the Swiss National Science Foundation, the Swiss Nanosciences Institute, the NCCR in Nanoscale Science, and the University of Basel for financial support. We thank Dr Ivana Císařová from the Charles University in Prague for the elemental analytical data on [Cu{(*R*,*R*)-**1**–2H}{Hg(ONO$_2$)$_2$}{Hg(ONO$_2$)}$_2$]$_n$.

References

1 E. C. Constable, G. Zhang, C. E. Housecroft, M. Neuburger, S. Schaffner, W.-D. Woggon and J. A. Zampese, *New J. Chem.*, 2009, **33**, 2166.
2 E. C. Constable, G. Zhang, C. E. Housecroft, M. Neuburger, S. Schaffner and W.-D. Woggon, *New J. Chem.*, 2009, **33**, 1064.
3 E. C. Constable, G. Zhang, C. E. Housecroft, M. Neuburger and S. Schaffner, *CrystEngComm*, 2009, **11**, 657.
4 E. C. Constable, G. Zhang, C. E. Housecroft, M. Neuburger and J. A. Zampese, *CrystEngComm*, 2010, DOI: 10.1039/b922929a, in press.
5 References cited in reference 4.
6 M. L. Colon, S. Y. Qian, D. Vanderveer and X. R. Bu, *Inorg. Chim. Acta*, 2004, **357**, 83.
7 R. Gheorghe, J.-P. Costes, S. Shova and M. Andruh, *Rev. Roum. Chim.*, 2007, **52**(8–9), 753.
8 See for example: L. Wang, X.-J. Zhu, W.-Y. Wong, J.-P. Guo, W.-K. Wong and Z.-Y. Li, *Dalton Trans.*, 2005, 3235; G. He, Y. Zhao, Y. Liu and C. Duan, *Inorg. Chem.*, 2008, **47**, 5169.
9 S. Thakurta, R. J. Butcher, G. Pilet and S. Mitra, *J. Mol. Struct.*, 2009, **929**, 112.
10 *Stoe & Cie, IPDS software v 1.26*, Stoe & Cie, Darmstadt, Germany, 1996.
11 G. M. Sheldrick, *Acta Crystallogr., Sect. A*, 2008, **64**, 112.
12 L. J. Farrugia, *J. Appl. Crystallogr.*, 1997, **30**, 565.
13 I. J. Bruno, J. C. Cole, P. R. Edgington, M. K. Kessler, C. F. Macrae, P. McCabe, J. Pearson and R. Taylor, *Acta Crystallogr., Sect. B: Struct. Sci.*, 2002, **58**, 389.
14 F. P. Gabbai, C. N. Burress, M.-A. Melaimi and T. J. Taylor, in *Comprehensive Organmetallic Chemistry III*, ed., D. M. P. Mingos and R. H. Crabtree, Elsevier, Oxford, 2007, Ch. 2.07, p. 419.
15 R. C. Larock, in *Comprehensive Organometallic Chemistry II*, ed., E. W. Abel, F. G. A. Stone and G. Wilkinson, Elsevier, Oxford, 1995, Ch. 9, p. 389.
16 T. Kajiwara, R. Murao and T. Ito, *J. Chem. Soc., Dalton Trans.*, 1997, 2537.
17 I. Ara, L. R. Falvello, J. Forniés, V. Sicilia and P. Villarroya, *Organometallics*, 2000, **19**, 3091.
18 N. K. Chawla and M. M. Jones, *Inorg. Chem.*, 1964, **3**, 1549.
19 R. J. Kline and J. G. Wardeska, *Inorg. Chem.*, 1969, **8**, 2153.
20 E. R. Schramm, W. Klapproth and F. H. Westheimer, *J. Phys. Colloid Chem*, 1951, **55**, 843.